PROCEEDINGS OF SCIENCE

ONLINE ICRC 2021
THE ASTROPARTICLE PHYSICS CONFERENCE
Berlin | Germany
37th International Cosmic Ray Conference
12–23 July 2021

Telescope Array Surface Detector Energy and Arrival Direction Estimation Using Deep Learning

O.E. Kalashev,[a,b,c,*] **D. Ivanov,**[d] **M.Yu. Kuznetsov,**[a,e] **G.I. Rubtsov,**[a] **T. Sako,**[f] **Y. Tsunesada**[g,h] **and Y.V. Zhezher**[a,f] **on behalf of the Telescope Array Collaboration**
(a complete list of authors can be found at the end of the proceedings)

[a] *Institute for Nuclear Research of the Russian Academy of Sciences, Moscow, 117312, Russia*
[b] *Moscow Institute for Physics and Technology, 9 Institutskiy per., Dolgoprudny, Moscow Region, 141701 Russia*
[c] *Novosibirsk State University, Pirogova 2, Novosibirsk, 630090 Russia*
[d] *High Energy Astrophysics Institute and Department of Physics and Astronomy, University of Utah, Salt Lake City, Utah, 84112-0830, USA*
[e] *Service de Physique Théorique, Université Libre de Bruxelles, Boulevard du Triomphe, CP225, 1050 Brussels, Belgium*
[f] *Institute for Cosmic Ray Research, University of Tokyo, Kashiwa, Chiba, 277-8582, Japan*
[g] *Graduate School of Science, Osaka City University, Osaka, Osaka, 558-0022, Japan*
[h] *Nambu Yoichiro Institute of Theoretical and Experimental Physics, Osaka City University, Osaka, Osaka, 558-8585, Japan*
E-mail: kalashev@inr.ac.ru

A novel ultra-high-energy cosmic rays energy and arrival direction reconstruction method for Telescope Array surface detector is presented. The analysis is based on a deep convolutional neural network using detector signal time series as the input and the network is trained on a large Monte-Carlo dataset. This method is compared in terms of statistical and systematic energy and arrival direction determination errors with the standard Telescope Array surface detector event reconstruction procedure.

**** 37th International Cosmic Ray Conference (ICRC2021), ****
**** 12-23 July 2021 ****
**** Berlin, Germany - Online ****

*Presenter

PoS(ICRC2021)252

1. Introduction

All current and planned ultra-high energy cosmic ray (UHECR) experiments detect cosmic rays indirectly by observing the extensive air showers (EAS) initiated by cosmic ray particles in the atmosphere. The largest statistics of the ultra-high energy EAS events is recorded by the networks of surface stations. The surface detector of the Telescope Array (TA) experiment [1, 2] is the largest one in the northern hemisphere. It covers the area over 700 km^2 in Utah, USA, with over 500 ground scintillation stations, placed at a distance of 1.2 km from each other in rectangular grid.

In TA SD the full time-resolved signal is recorded in two layers of each SD station scintillator. The standard SD event reconstruction [3] is built on fitting of the individual station readings with the predefined empirical functions. The event geometry is reconstructed using the arrival times of the shower front measured by the triggered stations. The shower front is approximated by the empirical functions first proposed by J. Linsley and L. Scarsi [4], then modified by the AGASA experiment [5] and fine-tuned to fit the TA data in a self-consistent manner. The integral signals of the individual stations are used to estimate the particle density at distance of 800 meters from the core S_{800} which plays a role of the lateral distribution profile normalization [6]. After the fit is performed, the primary particle energy is estimated as a function

$$E = E_{SD}(S_{800}, \theta)$$

of the density S_{800} at the distance of 800 m from the shower core and the zenith angle θ using the lookup table obtained with the Monte Carlo simulation [3]. In this work by means of machine learning methods we develop reconstruction procedure which allows to use the raw time-resolved signals directly. We show that the new approach lead to better event energy and arrival direction reconstruction accuracy.

2. Method

We use the full Monte Carlo simulation of TA SD events induced by the protons and nuclei described in details in Refs. [3, 7, 8]. We apply the standard energy spectrum and anisotropy reconstruction quality cuts [9] to the simulated events in the same way they are applied to the data. The full detector Monte Carlo simulation [3] of the TA observatory defines direct observables, time-resolved signals for the set of the adjacent triggered detectors, as a function of initial particle momentum. We use multi-layer feed-forward convolutional neural network (NN) [10], a well established machine learning algorithm to construct the inverse function. The choice of the convolutional architecture is motivated by the approximate translational symmetry of the inverse function with respect to detector grid location. The typical UHECR event triggers from 5 to 10 neighbour stations. For the purpose of energy and arrival direction reconstruction we found it enough to use the readouts from 4×4 grid of stations around the event core. Using 6×6 stations grid gives little improvement while requires at least factor of two more computation resources. The optimal neural network architecture is shown in Fig. 1. Each detector station records two time-resolved signals, one per layer, with 20 ns time resolution. Although for the most of events the signal length does not exceed 128 points we found it safe to use 256 points for the network input. The signal at each detector station is first converted to the vector of 28 features by the convolutional neural

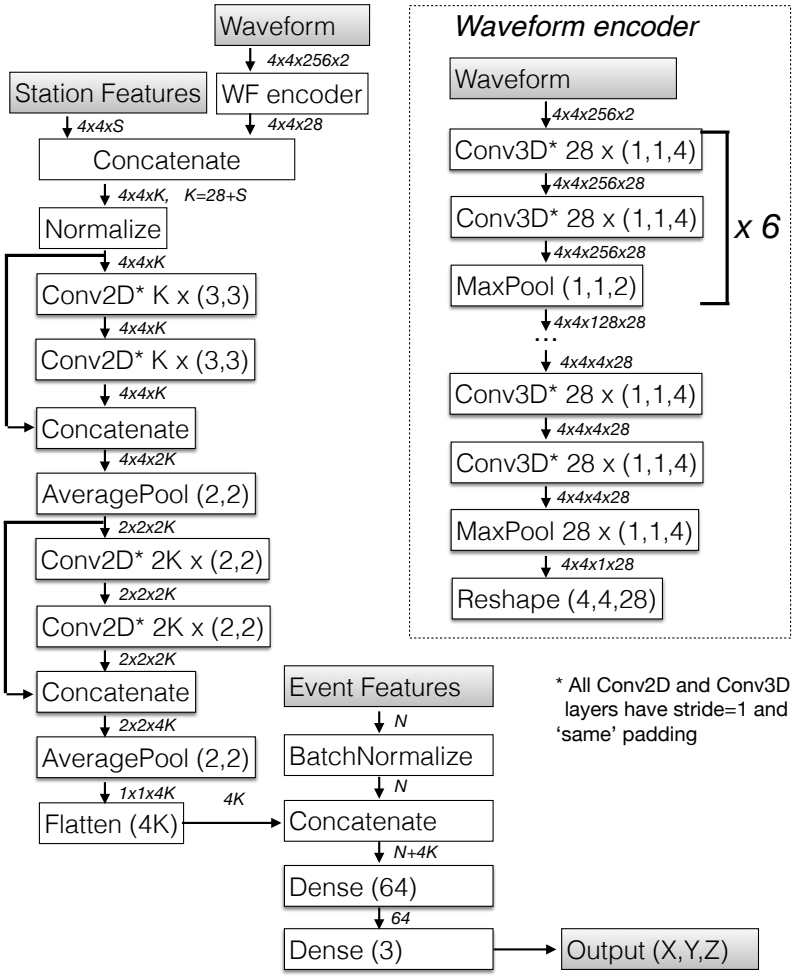

Figure 1: Neural network architecture

network model which we call waveform encoder. The raw waveform data is converted to the log scale before it is passed as an input to the encoder. Then extra detector features are added to the extracted feature vector including integral signal and waveform delay with respect to plane front obtained as a result of the standard event reconstruction as well as the detector station offset from the rectangular grid. The grid of extracted features is then processed as multichannel image by several convolutional layers followed by pooling until the image size is shrunk to $1x1$. In order to compensate the missing or disabled detectors, a special *Normalize* layer has been introduced, which drops the pixels corresponding to the missing detectors and multiplies the activations of the present detectors by a factor of $N_{total}/(N_{total} - N_{missing})$. Finally, the extracted event feature vector is concatenated with the external event features obtained by standard reconstruction procedure, e.g. S_{800} and a set of 14 composition sensitive synthetic observables [11]. The concatenated vector is then processed by 2-layer perceptron which outputs either 3 numbers being interpreted as a correction to the reconstructed coordinates of the arrival direction unit vector or just one number which is treated as a correction to the reconstructed initial particle energy logarithm. In both cases

we optimize the model weights by minimizing mean square error of the predicted quantity. The input and output data are normalized to have roughly zero mean and unit variance.

The model shown in Fig. 1 has about 120 thousand adjustable weights, which we optimize using the adaptive learning rate method Adadelta [12]. We split the data into training, test and validation parts with proportions 8 : 1 : 1 and perform gradient decent steps using training set for gradient calculation until the mean square error on the validation set reaches plateau which topically takes no more than 100 of training epochs. We found it enough to use just early stopping as the only regularization technique to avoid overfitting.

The NN model is implemented in *Python* using *Keras* [13] as a part of the *Tensorflow* library. We also use *Tune* library [14] along with hyperopt package [15] to optimize model hyperparameters, such as dimensionality of the waveform encoder output, the shapes of the convolution kernels and the dense layer size.

3. Energy reconstruction

As the first example of the event's NN-based event reconstruction enhancement we evaluate the event's energy E. In left Fig. 2 we compare the distributions of the energy reconstruction errors for standard and NN-enhanced reconstruction procedures using test data set with energy dependent event weights adjusted to fit HiRes experiment energy spectrum [16]. One can see that both the bias and the width of the distribution are smaller for the CNN reconstruction than the standard method. Note that the reconstruction procedures we discuss in this work are based on the Monte Carlo event set built using QGSJETII-03 hadronic interaction model. To illustrate the dependence of the primary particle energy reconstruction error on the interaction model we have generated additional MC event set using QGSJETII-04 model and applied both standard and NN-based reconstruction to the new event set. We see that error distribution, shown in right Fig. 2, has both smaller bias and width for NN-enhanced reconstruction, although the absolute bias values are now larger compared to QGSJETII-03 case, which is expected, since the whole procedure was optimized with QGSJETII-03.

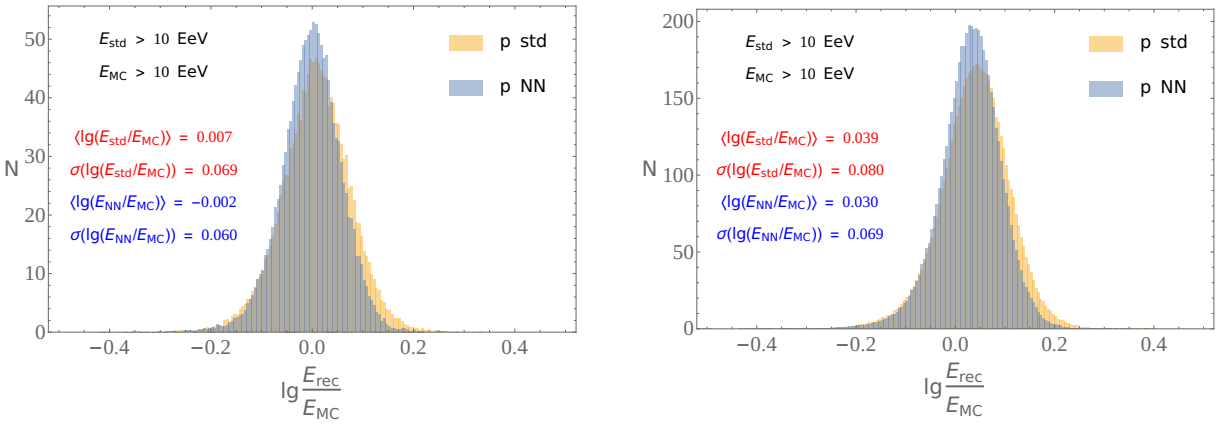

Figure 2: Distribution of the difference between the reconstructed and true values of an event's log energy for the standard (yellow histogram) and CNN-enhanced (blue histogram) reconstructions of the proton Monte Carlo event set simulated using QGSJETII-03 (left) or QGSJETII-04 (right) hadronic interaction model

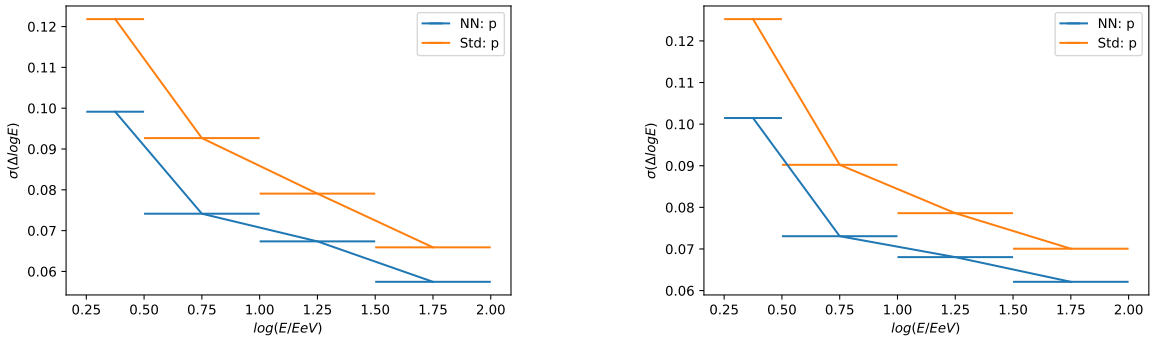

Figure 3: Standard deviation of the log energy reconstruction error calculated in four energy bins for the standard (orange curves) and CNN-enhanced (blue curves) reconstructions of the proton Monte Carlo event sets simulated using QGSJETII-03 (left plot) or QGSJETII-04 (right plots) hadronic interaction models.

In Fig. 3 we illustrate the energy dependence of the energy resolution. We show separately resolution obtained for test Monte Carlo event sets simulated using QGSJETII-03 (left plot) and QGSJETII-04 (right plots) hadronic interaction models. We see that for both cases the reconstruction accuracy grows with energy, with NN-based methods being more accurate in all energy bins. Namely, we get roughly 20% improvement in terms of log energy resolution which we get using NN-based reconstruction compared to standard one. We should remind, however, that changing hadronic interaction model also introduces some bias, which was not shown in the figure.

4. Arrival Direction Reconstruction

The NN-based reconstruction procedure outputs 3 components of unit vector pointing to the primary particle arrival direction. In Fig. 4 we convert it to zenith angle and evaluate the distribution of the zenith angle estimation errors for standard and NN-based reconstruction methods. We conclude that both the bias and the width of the distribution are smaller for the CNN reconstruction than the standard method.

In Fig. 5 we show distribution of angular distance between true and predicted direction obtained in standard and NN-based reconstructions for proton Monte-Carlo event set with event energies larger than 10 EeV and 57 EeV. We also calculate the angular resolution as 68% percentile of angular distance between true and reconstructed cosmic ray arrival direction.

Also as in previous section we estimate systematic uncertainty due to the choice of a particular hadronic interaction model by applying CNN reconstruction trained using QGSJETII-03 model to the test data set generated using QGSJETII-04 model. We plot angular resolutions for the proton and iron Monte Carlo event sets as a function of the reconstructed energy using either QGSJETII-03 or QGSJETII-04 hadronic interaction model for test data in Fig. 6. In both cases the training data was composed of Monte Carlo events initialized by H, He, N and Fe nuclei mixture in equal proportions calculated with QGSJETII-03 hadronic interaction model.

The angular resolution at a given energy is better on average for heavier nuclei since the EAS produced by heavy nuclei are typically wider and trigger more detectors. This seems to be the

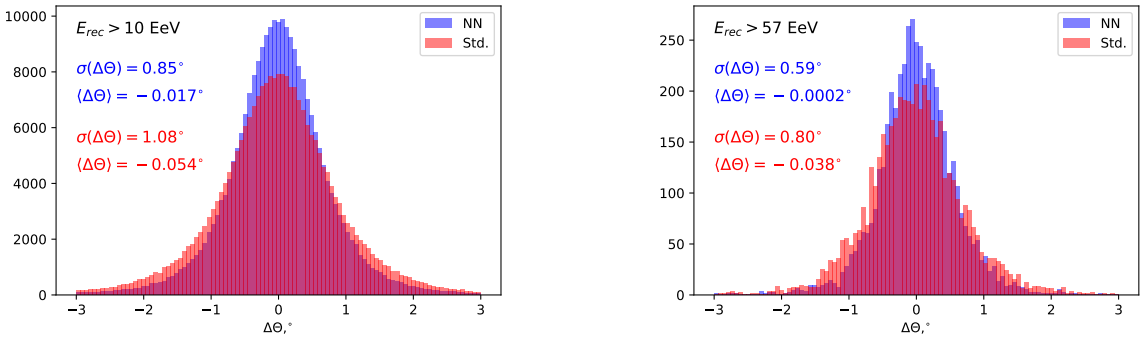

Figure 4: Distribution of the difference between the reconstructed and true values of an event's zenith angle for the standard (red histogram) and CNN-enhanced (blue histogram) reconstructions of the proton Monte Carlo event set simulated using QGSJETII-03 hadronic model for the reconstructed energy higher than 10 EeV (left figure) or 57 EeV (right figure).

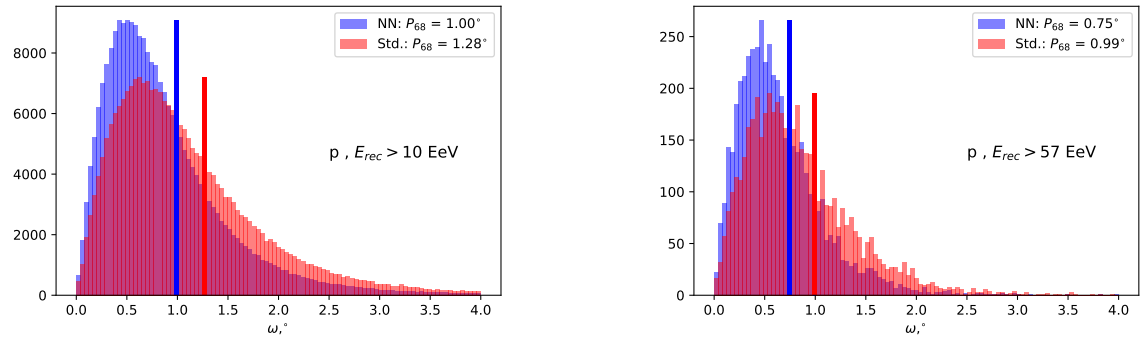

Figure 5: Angular distance ω distribution between the true and reconstructed arrival directions for the standard (red histogram) and CNN-enhanced (blue histogram) reconstructions of the proton Monte Carlo event set simulated using QGSJETII-03 hadronic model for the reconstructed energy higher than 10 EeV (left figure) or 57 EeV (right figure). Vertical lines denote the positions of 68% percentile of the distributions, i.e. the angular resolution values.

main reason of the resolution difference as it is clear from the Fig. 7 where the dependence of the resolution on the number of detectors triggered is shown for protons and iron nuclei.

5. Conclusions

We have shown that the deep learning based methods allow to substantially enhance the accuracy of the TA SD event energy and geometry reconstruction. The log energy resolution for proton showers was improved by about 20%, however this improvement has little effect on the possible systematic bias due to uncertainty in the hadronic interaction model.

The angular resolution for proton induced showers is improved from 1.35° to 1.07° at the primary energy of 1 EeV, from 1.28° to 1.00° at the primary energy of 10 EeV and from 0.99° to

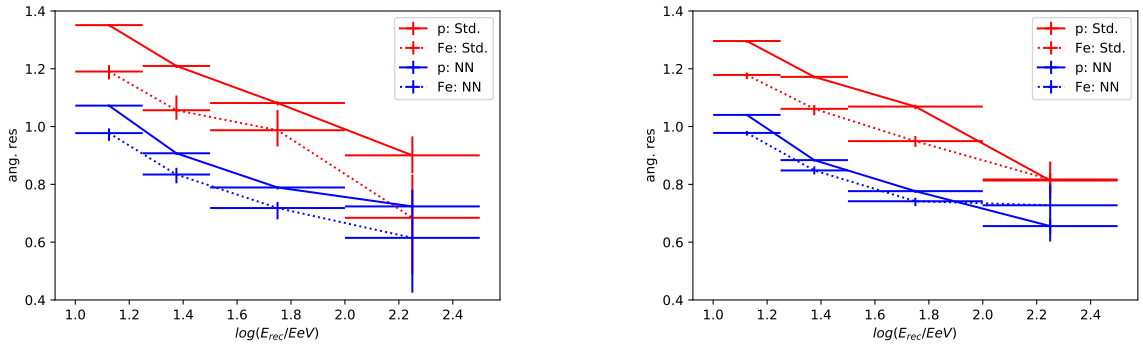

Figure 6: Angular resolution for the standard (red curves) and CNN-enhanced (blue curves) reconstructions of the proton (solid lines) and iron (dashed lines) Monte Carlo event sets simulated using QGSJETII-03 (left plot) or QGSJETII-04 (right plots) hadronic interaction models.

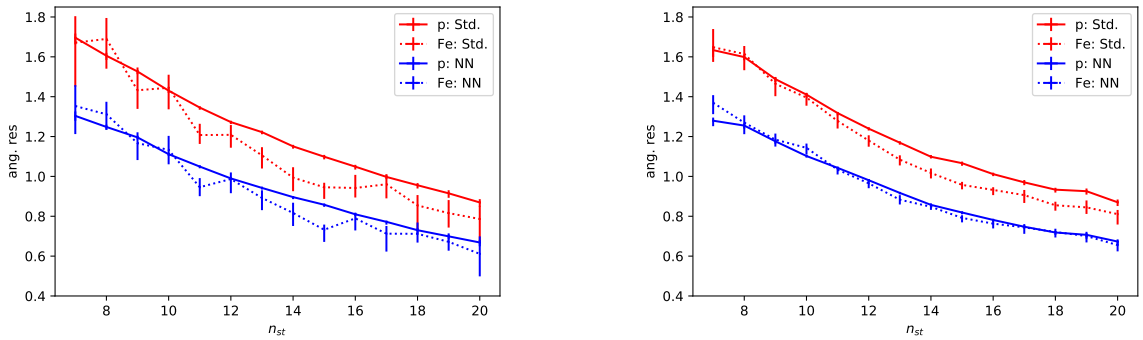

Figure 7: Angular resolution dependence on the number of detector stations triggered for the proton and iron Monte Carlo sets simulated using QGSJETII-03 (left plot) or QGSJETII-04 (right plot).

0.75° at the primary energy of 57 EeV. The result is especially important for the point source search, since background flux is proportional to the square of the angular resolution.

The systematic uncertainties related to the choice of hadronic interaction model which cause limited applicability of the new method for the primary particle energy determination seem to be almost irrelevant for the arrival direction reconstruction.

Acknowledgments

The cluster of the Theoretical Division of INR RAS was used for the numerical part of the work. The development and application of the machine learning analysis method is supported by the Russian Science Foundation grant No. 17-72-20291 (INR).

References

[1] Telescope Array collaboration, T. Abu-Zayyad et al., *The surface detector array of the Telescope Array experiment*, *Nucl. Instrum. Meth. A* **689** (2013) 87–97, [1201.4964].

[2] H. Tokuno et al., *New air fluorescence detectors employed in the Telescope Array experiment*, *Nucl. Instrum. Meth. A* **676** (2012) 54–65, [1201.0002].

[3] Telescope Array collaboration, T. Abu-Zayyad et al., *The Cosmic Ray Energy Spectrum Observed with the Surface Detector of the Telescope Array Experiment*, *Astrophys. J.* **768** (2013) L1, [1205.5067].

[4] J. Linsley and L. Scarsi, *Arrival times of air shower particles at large distances from the axis*, *Phys. Rev.* **128** (Dec, 1962) 2384–2392.

[5] M. Teshima et al., *Properties of 10**9-GeV - 10**10-GeV Extensive Air Showers at Core Distances Between 100-m and 3000-m*, *J. Phys.* **G12** (1986) 1097.

[6] M. Takeda et al., *Energy determination in the Akeno Giant Air Shower Array experiment*, *Astropart. Phys.* **19** (2003) 447–462, [astro-ph/0209422].

[7] Abu-Zayyad, T. and others, *CORSIKA Simulation of the Telescope Array Surface Detector*, *arXiv e-prints* (Mar, 2014) arXiv:1403.0644, [1403.0644].

[8] Telescope Array collaboration, J. Matthews, *Highlights from the Telescope Array Experiment*, *PoS* **ICRC2017** (2018) 1096.

[9] Telescope Array collaboration, D. Ivanov, *Energy Spectrum Measured by the Telescope Array*, *PoS* **358** (2019) .

[10] Y. LeCun, B. Boser, J. S. Denker, D. Henderson, R. E. Howard, W. Hubbard et al., *Backpropagation applied to handwritten zip code recognition*, *Neural Computation* **1** (Dec, 1989) 541–551.

[11] Telescope Array collaboration, R. U. Abbasi et al., *Mass composition of ultrahigh-energy cosmic rays with the Telescope Array Surface Detector data*, *Phys. Rev.* **D99** (2019) 022002, [1808.03680].

[12] M. D. Zeiler, *ADADELTA: an adaptive learning rate method*, *CoRR* **abs/1212.5701** (2012) , [1212.5701].

[13] F. Chollet et al., "Keras." https://github.com/fchollet/keras, 2015.

[14] R. Liaw, E. Liang, R. Nishihara, P. Moritz, J. E. Gonzalez and I. Stoica, *Tune: A research platform for distributed model selection and training*, *arXiv preprint arXiv:1807.05118* (2018) .

[15] Bergstra, J., D. Yamins, and D. D. Cox, *Making a Science of Model Search: Hyperparameter Optimizationin Hundreds of Dimensions for Vision Architectures.*, *JMLR Workshop and Conference Proceedings* **28(1)** (2013) 115–123.

[16] HiRes collaboration, R. U. Abbasi et al., *First observation of the Greisen-Zatsepin-Kuzmin suppression*, *Phys. Rev. Lett.* **100** (2008) 101101, [astro-ph/0703099].

The Telescope Array Collaboration

R.U. Abbasi[1], M. Abe[2], T. Abu-Zayyad[1,3], M. Allen[3], Y. Arai[4], E. Barcikowski[3], J.W. Belz[3], D.R. Bergman[3], S.A. Blake[3], I. Buckland[3], R. Cady[3], B.G. Cheon[5], J. Chiba[6], M. Chikawa[7], T. Fujii[8], K. Fujisue[7], K. Fujita[4], R. Fujiwara[4], M. Fukushima[7,9], R. Fukushima[4], G. Furlich[3], R. Gonzalez[3], W. Hanlon[3], M. Hayashi[10], N. Hayashida[11], K. Hibino[11], R. Higuchi[7], K. Honda[12], D. Ikeda[11], T. Inadomi[13], N. Inoue[2], T. Ishii[12], H. Ito[14], D. Ivanov[3], H. Iwakura[13], H.M. Jeong[15], S. Jeong[15], C.C.H. Jui[3], K. Kadota[16], F. Kakimoto[11], O. Kalashev[17], K. Kasahara[18], S. Kasami[19], H. Kawai[20], S. Kawakami[4], S. Kawana[2], K. Kawata[7], E. Kido[14], H.B. Kim[5], J.H. Kim[3], J.H. Kim[3], M.H. Kim[15], S.W. Kim[15], Y. Kimura[4], S. Kishigami[4], Y. Kubota[13], S. Kurisu[13], V. Kuzmin[17,a], M. Kuznetsov[17,21], Y.J. Kwon[22], K.H. Lee[15], B. Lubsandorzhiev[17], J.P. Lundquist[3,23], K. Machida[12], H. Matsumiya[4], T. Matsuyama[4], J.N. Matthews[3], R. Mayta[4], M. Minamino[4], K. Mukai[12], I. Myers[3], S. Nagataki[14], K. Nakai[4], R. Nakamura[13], T. Nakamura[24], T. Nakamura[13], Y. Nakamura[13], A. Nakazawa[13], T. Nonaka[7], H. Oda[4], S. Ogio[4,25], M. Ohnishi[7], H. Ohoka[7], Y. Oku[19], T. Okuda[26], Y. Omura[4], M. Ono[14], R. Onogi[4], A. Oshima[4], S. Ozawa[27], I.H. Park[15], M. Potts[3], M.S. Pshirkov[17,28], J. Remington[3], D.C. Rodriguez[3], G.I. Rubtsov[17], D. Ryu[29], H. Sagawa[7], R. Sahara[4], Y. Saito[13], N. Sakaki[7], T. Sako[7], N. Sakurai[4], K. Sano[13], K. Sato[4], T. Seki[13], K. Sekino[7], P.D. Shah[3], Y. Shibasaki[13], F. Shibata[12], N. Shibata[19], T. Shibata[7], H. Shimodaira[7], B.K. Shin[29], H.S. Shin[7], D. Shinto[19], J.D. Smith[3], P. Sokolsky[3], N. Sone[13], B.T. Stokes[3], T.A. Stroman[3], T. Suzawa[2], Y. Takagi[4], Y. Takahashi[4], M. Takamura[6], M. Takeda[7], R. Takeishi[7], A. Taketa[30], M. Takita[7], Y. Tameda[19], H. Tanaka[4], K. Tanaka[31], M. Tanaka[32], Y. Tanoue[4], S.B. Thomas[3], G.B. Thomson[3], P. Tinyakov[17,21], I. Tkachev[17], H. Tokuno[33], T. Tomida[13], S. Troitsky[17], R. Tsuda[4], Y. Tsunesada[4,25], Y. Uchihori[34], S. Udo[11], T. Uehama[13], F. Urban[35], T. Wong[3], K. Yada[7], M. Yamamoto[13], K. Yamazaki[11], J. Yang[36], K. Yashiro[6], F. Yoshida[19], Y. Yoshioka[13], Y. Zhezher[7,17], and Z. Zundel[3]

[1] Department of Physics, Loyola University Chicago, Chicago, Illinois, USA
[2] The Graduate School of Science and Engineering, Saitama University, Saitama, Saitama, Japan
[3] High Energy Astrophysics Institute and Department of Physics and Astronomy, University of Utah, Salt Lake City, Utah, USA
[4] Graduate School of Science, Osaka City University, Osaka, Osaka, Japan
[5] Department of Physics and The Research Institute of Natural Science, Hanyang University, Seongdong-gu, Seoul, Korea
[6] Department of Physics, Tokyo University of Science, Noda, Chiba, Japan
[7] Institute for Cosmic Ray Research, University of Tokyo, Kashiwa, Chiba, Japan
[8] The Hakubi Center for Advanced Research and Graduate School of Science, Kyoto University, Kitashirakawa-Oiwakecho, Sakyo-ku, Kyoto, Japan
[9] Kavli Institute for the Physics and Mathematics of the Universe (WPI), Todai Institutes for Advanced Study, University of Tokyo, Kashiwa, Chiba, Japan
[10] Information Engineering Graduate School of Science and Technology, Shinshu University, Nagano, Nagano, Japan
[11] Faculty of Engineering, Kanagawa University, Yokohama, Kanagawa, Japan
[12] Interdisciplinary Graduate School of Medicine and Engineering, University of Yamanashi, Kofu, Yamanashi, Japan
[13] Academic Assembly School of Science and Technology Institute of Engineering, Shinshu University, Nagano, Nagano, Japan
[14] Astrophysical Big Bang Laboratory, RIKEN, Wako, Saitama, Japan
[15] Department of Physics, Sungkyunkwan University, Jang-an-gu, Suwon, Korea
[16] Department of Physics, Tokyo City University, Setagaya-ku, Tokyo, Japan
[17] Institute for Nuclear Research of the Russian Academy of Sciences, Moscow, Russia
[18] Faculty of Systems Engineering and Science, Shibaura Institute of Technology, Minato-ku, Tokyo, Japan

[19] Department of Engineering Science, Faculty of Engineering, Osaka Electro-Communication University, Neyagawa-shi, Osaka, Japan
[20] Department of Physics, Chiba University, Chiba, Chiba, Japan
[21] Service de Physique Théorique, Université Libre de Bruxelles, Brussels, Belgium
[22] Department of Physics, Yonsei University, Seodaemun-gu, Seoul, Korea
[23] Center for Astrophysics and Cosmology, University of Nova Gorica, Nova Gorica, Slovenia
[24] Faculty of Science, Kochi University, Kochi, Kochi, Japan
[25] Nambu Yoichiro Institute of Theoretical and Experimental Physics, Osaka City University, Osaka, Osaka, Japan
[26] Department of Physical Sciences, Ritsumeikan University, Kusatsu, Shiga, Japan
[27] Quantum ICT Advanced Development Center, National Institute for Information and Communications Technology, Koganei, Tokyo, Japan
[28] Sternberg Astronomical Institute, Moscow M.V. Lomonosov State University, Moscow, Russia
[29] Department of Physics, School of Natural Sciences, Ulsan National Institute of Science and Technology, UNIST-gil, Ulsan, Korea
[30] Earthquake Research Institute, University of Tokyo, Bunkyo-ku, Tokyo, Japan
[31] Graduate School of Information Sciences, Hiroshima City University, Hiroshima, Hiroshima, Japan
[32] Institute of Particle and Nuclear Studies, KEK, Tsukuba, Ibaraki, Japan
[33] Graduate School of Science and Engineering, Tokyo Institute of Technology, Meguro, Tokyo, Japan
[34] Department of Research Planning and Promotion, Quantum Medical Science Directorate, National Institutes for Quantum and Radiological Science and Technology, Chiba, Chiba, Japan
[35] CEICO, Institute of Physics, Czech Academy of Sciences, Prague, Czech Republic
[36] Department of Physics and Institute for the Early Universe, Ewha Womans University, Seodaaemun-gu, Seoul, Korea

[a] Deceased